J. Fluid Mech. (1993), *vol.* 257, *pp.* 463–483

Experiments on isothermal and non-isothermal spreading

By PETER EHRHARD

Kernforschungszentrum Karlsruhe GmbH, Institut für Angewandte Thermo- und Fluiddynamik, Postfach 3640, D-76021 Karlsruhe, Germany

(Received 21 April 1992 and in revised form 23 June 1993)

Experiments are performed on axisymmetric spreading of viscous drops on glass plates. Two liquids are investigated: silicone oil (M-100), which spreads to 'infinity', and paraffin oil, which spreads to a finite-radius steady state. The experiments with silicone oil partly recover the behaviour of previous workers' data; those experiments with paraffin oil provide new data. It is found that gravitational forces dominate at long enough times while at shorter times capillary forces dominate. When the plate is heated or cooled with respect to the ambient gas, thermocapillary forces generate flows that alter the spreading dynamics. Heating (cooling) the plate is found to retard (augment) the spreading. Moreover, in case of partial wetting, the drop radius finally approached is smaller (larger) for a heated (cooled) plate. These data are all new. All these observations are in good quantitative agreement with the related model predictions of Ehrhard & Davis (1991). A breakdown of the axisymmetric character of the flow is observed only for very long times and/or very thin liquid layers.

1. Introduction

The spreading of liquids on solids is of interest in a variety of applications such as coating processes, cladding and soldering technology, and casting. In most of these applications non-isothermal conditions are present, leading to the occurrence of thermocapillary effects at the free interfaces. A spreading axisymmetric drop on a smooth horizontal plate subject to a non-isothermal temperature field thus exemplifies a problem of practical interest. From a scientific point of view the application of continuum mechanics in conjunction with the modelling of local microscopic effects at a contact line (contact of liquid, gas, solid) is likewise a challenging effort. It involves body forces due to gravity, surface forces at the liquid/gas interface due to mean-capillary and thermocapillary effects, line forces at the moving contact line as well as dissipative viscous forces, coupled within a free-boundary value problem.

There is a host of theoretical approaches to the modelling of spreading drops, subject to a variety of approximations and conditions. A review and classification of these models is given by Ehrhard & Davis (1991), who themselves develop a uniform model for the spreading of axisymmetric drops described above, by generalizing the approach of Greenspan (1978) to include (i) non-isothermal conditions, (ii) more general dynamic wetting behaviour and (iii) a consideration of vertically acting body forces. Their model will be employed in the present article to evaluate the experimental results. Conversely, the present experiments will be used to validate the theoretical predictions of Ehrhard & Davis.

There is a number of experimental studies available from the literature. Several experimentalists tackle the pure problem of moving contact lines in various geometric

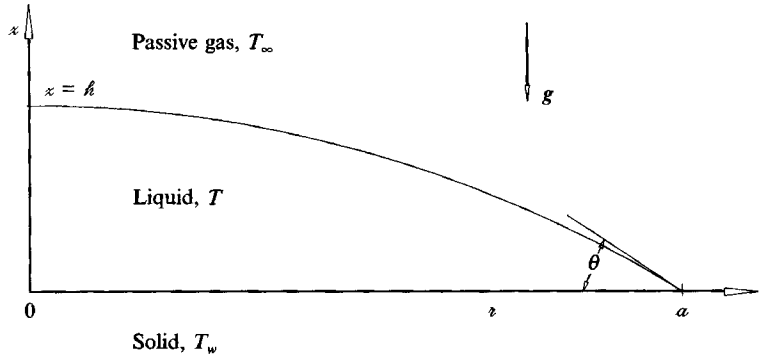

FIGURE 1. Sketch of the problem geometry.

configurations. Their results determine the dynamic wetting behaviour, encoded within the contact-angle-versus-speed characteristic $\theta = f(U_{cl})$, with various degrees of refinement (see e.g. Rose & Heins 1962; Friz 1965; Elliott & Riddiford 1967; Schwartz & Tajeda 1972; Hoffman 1975; Dussan V. 1979; de Gennes 1985). A detailed consideration of their findings is given in §3.2.

The isothermal spreading of liquid drops is the subject of a number of experimental investigations. Tanner (1979) conducted experiments on plane and axisymmetric silicone oil drops spreading on a smooth horizontal glass surface. He extracted spreading laws governed by capillary and viscous forces by considering an initial stage of the spreading process. A similar objective is the focus of the investigations of Chen (1988), who essentially confirmed Tanner's axisymmetric results for the capillary-dominated regime, using silicone oil on glass. A combined experimental study on both capillary-dominated and gravity-dominated regimes was performed by Cazabat & Cohen Stuart (1986). They used silicone oils of various viscosities on a horizontal glass surface to study axisymmetrically spreading drops. Their results provide spreading laws for both regimes as well as information on the transition times, depending on various parameters. In a recent paper Levinson *et al.* (1988) addressed silicone oil drops hanging below a horizontal glass plate and, thus, obtained spreading laws for conditions where gravitational forces are inverted.

There is very little work in the literature related to non-constant surface tension within this context. Carles & Cazabat (1989) studied drops in an atmosphere saturated with a volatile compound. Owing to soluto-capillary effects, they observed strongly accelerated spreading and wavy, three-dimensional instabilities at the drop circumference.

The present article aims to study experimentally the spreading of liquid drops of silicone oil and paraffin oil on smooth horizontal plates under isothermal and non-isothermal conditions. In detail, we investigate the following. (i) The isothermal spreading of silicone oil and observe, consistently with findings by other authors, unlimited spreading in conjunction with a mobility exponent of $m \approx 2.8$. (ii) The isothermal spreading of paraffin oil which yields limited spreading – these results are new. Finally, we address the non-isothermal spreading of (iii) silicone oil and (iv) paraffin oil and find that thermocapillary forces have a profound effect on the spreading. Likewise, these results are new. All experiments in groups (i–iv) compare well with theoretical predictions of Ehrhard & Davis (1991). Additionally, several earlier isothermal experiments by other authors, using silicone oil (group i), are included in a careful comparison.

2. Problem and model

We consider the spreading of an axisymmetric drop on a smooth horizontal rigid plane, which is kept at a constant temperature T_w. The drop is composed of a non-volatile Newtonian liquid and surrounded by a passive gas whose far-field temperature is T_∞. The geometry is sketched in figure 1. The shape of the interface between the spreading liquid and the ambient gas is given by $z = h$, the contact-line position is given by $r = a$, and the contact angle is denoted by θ.

Ehrhard & Davis (1991) have examined such a system and, using lubrication theory and a small-mobility-capillary-number (small-C) approximation, obtain a dimensionless evolution equation for the drop shape $h(r, t)$. We summarize the conditions and assumptions used in deriving this model. The quasi-steady evolution equation for the drop shape appropriate to small C,

$$\frac{1}{r}\left\{\tfrac{1}{3}h^3 r\left(h_{rr}+\frac{1}{r}h_r-Gh\right)_r+\tfrac{1}{2}Mh^2rh_r\right\}_r=0, \tag{2.1}$$

is linked initially ($t = 0$) with the following boundary and side conditions:

$$\left.\begin{gathered} h(r,0)=h_0(r),\quad h_0(1)=0,\quad a(0)=1,\\ h_{0r}(0)=0,\quad \lim_{r\to 0}(rh_{0rrr}(r))=0,\\ h_{0r}(1)=-1/V,\\ 2\pi\int_{r=0}^{1} rh_0(r)\,\mathrm{d}r=1. \end{gathered}\right\} \tag{2.2}$$

During the evolution of the drop ($t > 0$) we have the boundary and side conditions:

$$\left.\begin{gathered} h(a,t)=0,\\ h_r(0,t)=0,\quad \lim_{r\to 0}(rh_{rrr}(r,t))=0,\\ h_r(a,t)=-\Theta(t),\\ 2\pi\int_{r=0}^{a(t)} rh(r,t)\,\mathrm{d}r=1. \end{gathered}\right\} \tag{2.3}$$

The above sets of conditions (2.2) and (2.3) retain symmetry and smoothness of the drop shape and ensure constant liquid volume. The instantaneous contact angle $\Theta(t)$ depends on the speed a_t of the contact line as follows:

$$\Theta(t)=(a_t(t))^{1/m}+\Theta_A. \tag{2.4}$$

For the above set of equations (2.1)–(2.4) Ehrhard & Davis have employed the following set of dimensionless variables (the rescaling is described in the Appendix):

$$\left.\begin{gathered} r=\frac{r}{a_0},\quad z=\frac{z}{a_0\theta_0 V},\quad t=\frac{\kappa\theta_0^m V^m}{a_0}t,\\ \Theta=\frac{\theta}{\theta_0 V},\quad V=\frac{\mathscr{V}_0}{a_0^3\theta_0}. \end{gathered}\right\} \tag{2.5}$$

The evolution equation (2.1) involves certain dimensionless groups, namely the

mobility capillary number C, the Bond number G and the effective Marangoni number M, defined by

$$C = \frac{\mu\kappa}{\sigma_w \theta_0^{(3-m)} V^{(3-m)}}, \quad G = \frac{\rho g a_0^2}{\sigma_w}, \quad M = \frac{\sigma_w - \sigma_\infty}{\sigma_w} \frac{a_0 \lambda_\infty}{V \theta_0 \delta\lambda}. \tag{2.6}$$

Herein μ, λ, σ_w, σ_∞ are the properties of the spreading liquid, namely viscosity, heat conductivity, and surface tension towards the ambient helium at temperatures T_w and T_∞, respectively. Further a_0, θ_0, V_0 are the initial data for an individual drop, namely the radius, contact angle and volume. λ_∞ is the heat conductivity of the ambient gas and δ the thickness of the thermal boundary layer established above the drop. The contact-line relation (2.4) comes from the dimensional characteristic relating the contact-line speed U_{cl} to the contact angle θ,

$$U_{cl} = \kappa(\theta - \theta_A)^m. \tag{2.7}$$

Herein $m \geqslant 1$ is the so-called mobility exponent, $\kappa > 0$ is an empirical constant and $\theta_A \geqslant 0$ is the (static) advancing contact angle. Note that we employ script lettering for physical quantities and italic for dimensionless quantities.

The above dimensionless groups describe the relative importance of various physical mechanisms. The mobility capillary number C measures the ratio of the initial mobility speed $\kappa\theta_0^m$ to the speed given by viscous forces and mean surface tension. The Bond number G relates gravitational forces and mean surface tension and thus allows us to judge the significance of gravity. The Marangoni number M provides a measure of the relative importance of thermocapillary effects with respect to mean capillary effects. It involves quantities which determine the heat transfer at the liquid/gas interface. For $M > 0$ ($M < 0$) the plate is heated (cooled) with respect to the ambient gas.

The assumptions and approximations used to derive the above model might be summarized as follows:

(i) A slip law is posed to relieve the contact-line singularity.

(ii) The plate is isothermal and the heat transfer at the liquid/gas interface is modelled by a heat transfer coefficient measured by the Biot number B,

$$B = a_0 \theta_0 \lambda_\infty V/\delta\lambda. \tag{2.8}$$

$B \ll 1$ since the interface is nearly adiabatic.

(iii) The interface surface tension is linear in temperature.

(iv) Lubrication theory (for thin drops) is employed so that $\theta_0 \ll 1$ as usual; the mobility capillary number is small.

(v) In the analysis of the evolutionary system (2.1)–(2.3), $C \to 0$ so that the spreading is limited by the mobility of the contact line (and not by slippage); equation (2.1) thus has no time derivative. In this case at leading order in C, the slip coefficient that would normally appear in (2.1) may be set to zero.

Based on the above summary of the model by Ehrhard & Davis (1991) we use that model for a set of simulations demonstrating the influence of the temperature field. Figure 2 shows the evolution of the drop shape for three typical situations, namely a cooled plate ($M = -0.05$), an isothermal plate ($M = 0$) and a heated plate ($M = 0.2$). The initial and subsequent drop contours are plotted in time steps of $\Delta t = 0.4$. We clearly see the effect of the temperature field on the development of the drop. For a cooled (heated) plate the spreading is augmented (retarded) with respect to the isothermal case. The drop contour for $t \to \infty$, which is given by the dashed lines, is flatter (steeper) if the plate is cooled (heated). The above phenomena are caused by thermocapillary-driven flows within the drop, which alter the pure-spreading flow field

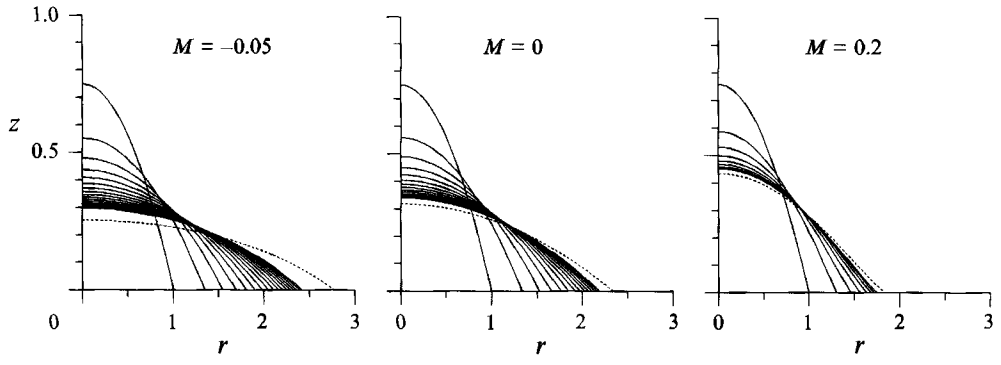

FIGURE 2. Evolution of the drop shape $h(r, t)$ as predicted for various thermal conditions. Parameters are $G = 0$, $\Theta_A = 0.25$, $m = 2.8$, a time step of $\Delta t = 0.4$ is used to create a number of successive contours. Dashed contours are obtained for $t \to \infty$.

present in the isothermal situation. Note that owing to the separate scalings of the two spatial coordinates, a thin drop with $a \gg h$ in real dimensions, appears strongly stretched in dimensionless coordinates r, z. Thus figure 2 shows thin drops.

3. Experimental methods

We aim to assess experimental data for spreading drops subject to a variety of thermal conditions. We mainly concentrate, in this first experiment on non-isothermal spreading, on the measurement of the wetted area underneath the drop. For this purpose we apply an optical schlieren-type technique. We also need to establish extremely carefully controlled thermal conditions. These are the main ideas leading to the following set-up and methods.

3.1. *Set-up of the experiment*

Figure 3 illustrates the experimental set-up. The actual experiment takes place within a closed Plexiglas cylinder of 200 mm in diameter, where the spreading drop (silicone oil or paraffin oil) is placed upon a temperature-controlled glass surface. The drop is positioned using an injection needle, and its mass is determined to an accuracy of ± 1 μg by difference weighing using a precision scale.

The horizontal surface on which the spreading takes place is composed of a copper cylinder 130 mm in diameter covered on top by a thin glass plate. The copper cylinder is kept at constant temperature T_w by circulating coolant (accuracy ± 0.1 °C). The glass plate is 160 μm in thickness and is held by adhesive forces provided by a thin oil film between glass plate and copper cylinder. Thus an intimate contact is established which guarantees several advantages. (i) The 'flexible' glass plate is kept at a precisely plane position attached to the top of the copper cylinder. (ii) A reproducible smooth surface is provided with defined chemical properties. (iii) A perfectly conducting thermal boundary condition is approximately realized. The effect of the glass plate and the oil film on the thermal boundary conditions has been checked by calculating temperature profiles across those layers for typical heat fluxes. We find that the temperature difference across the added layers is always less than 2% of the total applied temperature difference $T_w - T_\infty$. Thus, the perfectly conducting boundary condition provided by the copper cylinder is maintained to a reasonable degree. The experimental

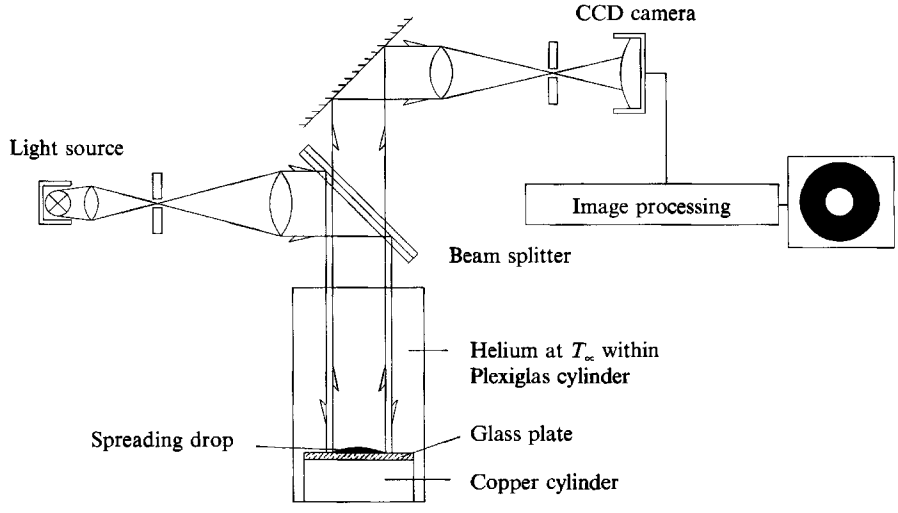

FIGURE 3. Sketch of the experimental set-up.

module described above can be adjusted to a horizontal position by means of three micrometer screws and a precision gauge.

Helium is chosen as the ambient gas within the Plexiglas cylinder because of its high heat conductivity λ_∞, which enforces thermal effects. To provide a constant helium temperature T_∞ for non-isothermal situations, i.e. for $T_w \neq T_\infty$, it is necessary to set up a flow inside the ambient helium together with an adequate temperature control. During the spreading process we establish a weak stagnant point flow entering radially at the top of the Plexiglas cylinder and proceeding vertically downwards towards the horizontal glass plate. The helium leaves the Plexiglas cylinder through the coaxial gap between the copper and Plexiglas cylinders. We use an average axial velocity of $\bar{u} \approx 10$ mm/s for the flow in the Plexiglas cylinder while just above the drop we expect a radially directed flow with significantly lower velocities. We have double-checked very carefully the ambient helium flow with respect to the development of distortions of the liquid flow inside the drop. During preliminary measurements we sought the 'critical gas flow rate' which causes the first evident changes in the isothermal spreading laws. Later, the gas flow rate is set at 25% of this 'critical' rate.

The helium entering the experimental volume is conditioned at a temperature T_∞ and, additionally, inside the Plexiglas cylinder copper sheets at the circumference are kept at T_∞ by circulating coolant. Thus the helium hits the glass plate with a fairly well-defined temperature, whereas temporal fluctuations may have amplitudes up to ± 0.5 °C for an applied temperature span of $T_w - T_\infty = \pm 25$ °C. Three PT-100 resistor thermometers monitor the temperatures of the ambient helium T_∞ at two locations in a horizontal plane 5 mm above the glass plate, and T_w at the top surface of the copper cylinder. The accuracy of the temperature measurements is ± 0.01 °C.

The optical measurement of the wetted area $\mathscr{A}(t)$ is based on a schlieren system using reflection. We use a mercury-vapour light source together with a spatial filter and various lenses to provide a parallel beam of 10 cm in diameter. This parallel light enters the test section vertically through a glass cover. After reflection at the drop and the glass plate, respectively, the light passes through a beam splitter to be spatially filtered by a pin-hole in the Fourier plane. A square-pixel CCD camera finally records the image for further digital processing.

Material properties	Silicone oil	Paraffin oil
Viscosity, μ (10^{-3} Pa s)	$200.98-3.615T+0.024T^2$	$408.70-18.75T+0.25T^2$
Surface tension, σ (N m^{-1})	$20.465-0.045T$	$28.938-0.179T$
Density, ρ (kg m^{-3})	$999.18-1.144T+0.0025T^2$	$899.67-1.0T$
Heat conductivity, λ (W m^{-1} K^{-1})	0.163 (for $T \approx 25$ °C)	0.130 (for $T \approx 25$ °C)

TABLE 1. Material properties used, where T is in units of °C. For helium at $T \approx 25$ °C, $\lambda = 0.150$ W m^{-1} K^1

The above technique takes advantage of the following physics. The unwetted glass plate, as well as the middle region of the drop, reflect the light in a parallel manner. This parallel light passes through the low-pass filter in the Fourier plane and is recorded by the CCD camera as bright. In contrast, non-parallel reflected light from the outer inclined drop surface areas is stopped by the filter and appears dark. Thus, we obtain a high-contrast picture of the drop as shown schematically in figure 3. Subsequent image processing accepts the outer contour as the circumference of the drop. The number of pixels inside this closed contour is determined and, together with an initial calibration, a highly accurate measurement of the wetted area $\mathscr{A}(t)$ is inferred. The relative error of the area measurement proves to be less than 0.1%. From $\mathscr{A}(t)$ the radius $a(t)$ is calculated by assuming a circular shape.

During the whole measuring protocol we consider three different thermal conditions: (I) an isothermal situation, $T_w = T_\infty$; (II) a heated plate, $T_w - T_\infty = +25$ °C; (III) a cooled plate, $T_w - T_\infty = -25$ °C. Thereby, the plate temperature, which is closely linked to the average liquid temperature, is always kept at $T_w = +25$ °C. This allows us to maintain the thermophysical properties of the spreading liquid constant to a reasonable degree for all cases I–III. Note that cases II and III represent two symmetric situations with the plate being heated (cooled) by identical temperature spans above (below) the ambient helium temperature.

We use two different liquids, namely silicone oil Bayer M-100 and paraffin oil in our experiments. A new glass plate is prepared and fixed onto the copper cylinder for each drop. The preparation of the glass plate depends on the test liquid. In the case of silicone oil the plate is cleaned using ethanol in an ultrasonic bath for about 10 minutes. The glass plates are kept afterwards for at least two days within a dust-free container to ensure complete evaporation of the ethanol. In the case of paraffin oil an identical procedure is followed using distilled water instead of ethanol. The dynamic wetting behaviour of these liquids on glass prepared like this will be discussed in the following subsection.

3.2. *Scaling and preliminary measurements*

In order to allow a comparison of various test liquids and model predictions we apply the scaling laws (2.5), (2.6) to the experimental data. In (2.5), (2.6) there are several quantities which need to be fixed during preliminary measurements or from limiting behaviour. In this subsection these methods are explained.

We have determined the dependence of various properties such as surface tension $\sigma(T)$, viscosity $\mu(T)$ and density $\rho(T)$ of our test fluids within the appropriate temperature range. Those data are summarized in table 1 and used for all scalings and dimensionless groups.

The measurement of the initial contact angle θ_0 and the mobility capillary number C allows us to assess whether the assumptions of the theory, namely the lubrication approximation ($\theta_0 \ll 1$) and the small-mobility-capillary-number approximation

($C \ll 1$), are adequately satisfied. The initial contact angle θ_0 of each drop is estimated from its volume $\mathcal{V}_0$ (from mass measurement) by assuming a spherical cap. We vary the initial contact angle θ_0 in the range

$$6.9° \leqslant \theta_0 \leqslant 18.3° \quad \text{for silicone oil/glass,} \tag{3.1}$$

$$12.8° \leqslant \theta_0 \leqslant 20.3° \quad \text{for paraffin oil/glass.} \tag{3.2}$$

The mobility capillary numbers C are in the range

$$0.53 \times 10^{-2} \leqslant C \leqslant 8.20 \times 10^{-2} \quad \text{for silicone oil/glass,} \tag{3.3}$$

$$0.59 \times 10^{-2} \leqslant C \leqslant 2.72 \times 10^{-2} \quad \text{for paraffin oil/glass.} \tag{3.4}$$

Clearly, the range of mobility capillary numbers proves the quasi-steady approach ($C \to 0$) to be a good approximation, while the lubrication approximation might lead to inaccuracies due to initial contact angles of up to $\theta_0 \approx 0.35$.

The lubrication approximation is appropriate here in view of the range of contact angles considered (cf. (3.1), (3.2)). Goodwin & Homsy (1991) show for the related problem of a liquid sheet with contact line on an inclined plane that results with the lubrication approximation compare well with those from a numerical solution of the Stokes equations as long as the contact angle is small enough. By tracking 'a representative functional' with capillary number (cf. figure 12 in their paper) they demonstrate predictions, for example for the slope of their particular macroscopic quantity, to be accurate to $\pm 2\%$ in a surprisingly wide range of contact angles $0 \leqslant \theta \leqslant 50°$ if lubrication approximation is used. Of course, any dependency of results on contact angle is shown to be lost. Thus, for the present problem a reasonably accurate model should result from the lubrication approximation, in particular since large contact angles are present only at very early stages of the spreading and decrease rapidly as time progresses.

The determination of the Marangoni number M requires us to quantify the heat transfer conditions at the liquid/helium interface, encoded within the thermal boundary-layer thickness δ. For that reason we determine for two cases, namely $T_w - T_\infty = \pm 25$ °C, the vertical temperature profiles above the spreading drop using a 0.25 mm diameter thermocouple. In detail we traverse the thermocouple vertically in steps $\Delta z = 0.2$ mm and measure at each position the time-averaged helium temperature. From those temperature profiles above the liquid, we find a roughly linear increase/decrease over a thermal boundary-layer of thickness in a range 0.6–1.0 mm. Estimating the heat flux on the basis of conduction in the thermal boundary layer, the Marangoni numbers M are respectively:

$$T_w - T_\infty = +25\ °\text{C}: \quad M \approx +0.085, \tag{3.5}$$

$$T_w - T_\infty = -25\ °\text{C}: \quad M \approx -0.06, \tag{3.6}$$

for both silicone oil and paraffin oil. Equations (3.5) and (3.6) confirm, from their order of magnitude, the near-adiabatic thermal boundary condition at the liquid/helium interface. It should be kept in mind, however, that this method does not allow for a precise non-intrusive measurement of local temperatures within the helium. In particular the heat flow inside the probe and temperature oscillations of the helium, most evident for the unstable profile $T_w > T_\infty$, introduce major errors besides the standard error of pure temperature measurements (± 0.01 °C). Thus, values given in (3.5) and (3.6) are estimates and their order of magnitude only can be used with confidence.

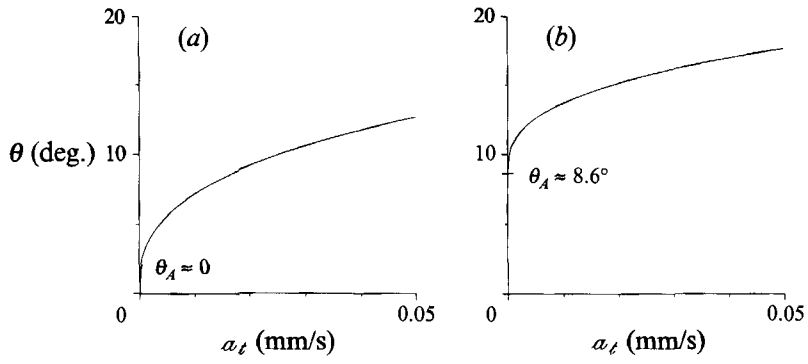

FIGURE 4. Wetting behaviour on glass of the liquids used in the experiments, as determined by indirect measurements: (*a*) silicone oil, (*b*) paraffin oil.

The dynamic wetting behaviour in dimensional form is encoded within the constitutive equation (2.7) with $U_{cl} = a_{,t}$,

$$a_{,t} = \kappa(\theta - \theta_A)^m. \tag{3.7}$$

We take an indirect approach to determine the constants in (3.7). The advancing (static) contact angle θ_A is estimated from the final drop size. In detail we find for silicone oil that no steady state exists as $t \to \infty$, and therefrom $\theta_A \approx 0$. In contrast, the paraffin oil experiments lead to a steady drop shape as $t \to \infty$, which allows an identification of the advancing contact angle in an accuracy range $6.8° \leqslant \theta_A \leqslant 9.2°$. The average value $\bar{\theta}_A \approx 8.6°$, is used henceforth.

The mobility exponent m is determined using the isothermal silicone oil experiments. As $t \to \infty$ those drops follow to a good approximation the law

$$t \to \infty: \quad a \propto t^c, \tag{3.8}$$

while the model of Ehrhard & Davis (1991) predicts for isothermal axisymmetric drops under gravity the behaviour

$$t \to \infty: \quad a \propto t^{\frac{1}{(2m+1)}}. \tag{3.9}$$

Therefore, regressing the experimental data to the model (3.8) allows the mobility exponent m to be identified. We find a narrow range of $2.64 \leqslant m \leqslant 2.95$ and henceforth use the average value $\bar{m} = 2.8$. Although the determination of the mobility exponent has been performed using the silicone oil experiments, it defines the type of functional dependency in (3.7). Since the underlying physics is not changed when silicone oil is replaced by paraffin oil, we assume the same type of functional dependency, and so the same mobility exponent for paraffin oil on glass. For given θ_0, θ_A, m the constant κ in (3.7) can be derived from the measured radius $a(t)$ by differentiation, i.e.

$$\kappa = \frac{a_{,t}(t_0)}{(\theta_0 - \theta_A)^m}. \tag{3.10}$$

From this equation κ is found to be

$$\kappa = 3.4 \times 10^{-3}\ \text{m/s} \quad \text{for silicone oil/glass}, \tag{3.11}$$

$$\kappa = 8.7 \times 10^{-3}\ \text{m/s} \quad \text{for paraffin oil/glass}. \tag{3.12}$$

We summarize the data obtained for the dynamic-wetting behaviour by presenting the corresponding functions graphically. In figure 4 the contact angle θ is plotted as a function of the (advancing) speed of the contact line $a_{,t}$ for both silicone oil on glass

(*a*) and paraffin oil on glass (*b*). It should be kept in mind that these laws have not been obtained by direct measurements. The consistency of this method will be confirmed below.

Our indirect findings concerning the dynamic wetting behaviour of these two liquids on glass can be supported by direct investigations on the dynamic contact angle conducted by other authors. De Gennes (1985), citing experiments by Hoffman (1975), concludes that the functional form of $\theta = f(a_\ell)$ should be universal and independent of the choice of materials. Moreover, Hoffman's experiments suggest a model of type (3.7) for both complete wetting ($\theta_A = 0$) and partial wetting ($\theta_A > 0$). For small speeds of the contact line his data yield a mobility exponent of $m = 3.0 \pm 0.5$ (see de Gennes). Likewise, Rose & Heins (1962), Friz (1965) and Schwartz & Tajeda (1972) propose from their experimental data and physical reasoning that

$$\tan\theta \approx 3.4\left(\frac{a_\ell \mu}{\sigma}\right)^{\frac{1}{3}}, \tag{3.13}$$

where, additionally, a dependence on dynamic viscosity μ and surface tension σ is obtained. For $\theta \ll 1$, (3.13) recovers a mobility exponent of $m = 3$ for cases of complete wetting. Calculating the constant κ in (3.7) via (3.13) gives

$$\kappa = 3.95 \times 10^{-3}\ \text{m/s} \quad \text{for silicone oil/glass,} \tag{3.14}$$

$$\kappa = 6.47 \times 10^{-3}\ \text{m/s} \quad \text{for paraffin oil/glass,} \tag{3.15}$$

which compares reasonably well with our indirect findings (3.11), (3.12).

There is a recent theoretical article by Hocking (1992) that likewise supports the use of the mobility exponent $m = 3$. Starting from the dual assumptions of some form of slip at the contact line and the contact angle being always identical with the static contact angle (on a microscopic scale), he concludes that the dynamic variation of the apparent contact angle should be proportional to $a_\ell^{\frac{1}{3}}$. Of course, the expression 'contact angle' throughout the present article has to be identified with 'apparent contact angle' in Hocking's terms. Again therefrom $m = 3$ is readily inferred.

Besides these more general findings on contact-line dynamics there are measurements directly related to our liquids. Hoffman's experiments include measurements of the advancing dynamic contact angle for silicone oil in a glass capillary tube. These data are in excellent agreement with our indirect findings. Rose & Heins took measurements for paraffin oil using a similar glass–tube geometry. Their data confirm $\theta_A \approx 10°$ as well as the functional dependency of the contact angle on the speed of the contact line. Concerning some discrepancies within the data for paraffin oil with respect to the precise values of κ and θ_A, we stress that both the experiment of Rose & Heins and our indirect measurements exhibit considerable scatter of the data. Thus, in contrast to the silicone oil case, a more precise determination is not really possible from those measurements.

4. Results for silicone oil/glass: unlimited spreading

From the dynamic-wetting behaviour of silicone oil on glass, shown in figure 4(*a*), it can be concluded that, given an initial contact angle $\theta_0 > 0$, a drop will spread ($a_\ell > 0$) and therefore decrease its actual contact angle θ as time progresses. Since $\theta_A \approx 0$, every positive contact angle θ will correspond to a speed $a_\ell > 0$, and hence the drop will spread forever. This behaviour is attributed to cases $\theta_A \approx 0$ and is typically observed for spreading of silicone oil on glass. In the following sections we firstly present isothermal spreading results for this case. This demonstrates the ability of our

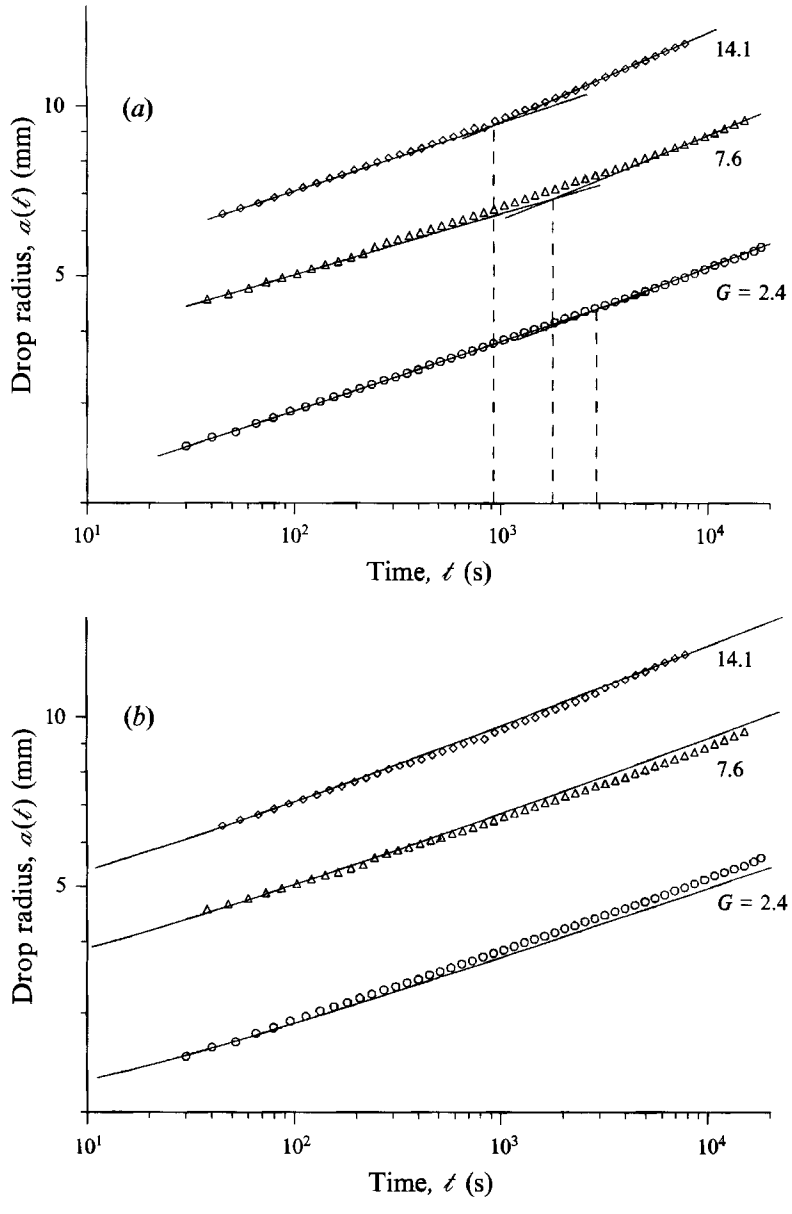

FIGURE 5. Isothermal spreading of silicone oil on glass, the perfectly wetting system: drop radius as function of time for three drops of different volumes. (*a*) Experimental data and regression curves therefrom, (*b*) experimental data and model predictions.

overall experimental procedure to recover experimental observations reported by other investigators. A careful comparison is conducted. Secondly, results for non-isothermal conditions are presented. These types of experiments have never been performed before and thus give new results.

4.1. *Isothermal conditions*

In figure 5 we show the development of three typical single drops of different volumes $\mathscr{V}_i$, obtained under isothermal conditions, i.e. $T_w = T_\infty (M = 0)$. The drop radius a is plotted as a function of time t, in double-logarithmic coordinates. From the definition

(2.6) of the Bond number G we can infer three different Bond numbers G_i for three different initial radii $a_{0,i}$. In particular the Bond number increases quadratically with the initial drop radius, implying that gravitational forces are more important for large drops than for small drops. This interrelation is reflected by the growth behaviour of the drops shown in figure 5. From the regression of the experimental data of each drop for both small and large times we obtain

$$t \to 0: \quad a \propto t^{c_0}, \tag{4.1}$$

$$t \to \infty: \quad a \propto t^{c_\infty}, \tag{4.2}$$

with $c_0 < c_\infty$. These experimental regression results for both small and large times are incorporated in figure 5(*a*). They indicate that a transition occurs from an initially small slope towards a larger slope as t increases. The different slopes can be attributed to the different effects that control the process as discussed by Ehrhard & Davis (1991). At small times capillary forces are dominant, causing a smaller slope c_0. As the drop develops, the height approaches zero and the interface curvature tends to infinity. Therefore, at large times gravitational forces control the process, causing a larger slope c_∞. One would thus expect this transition to occur earlier when the Bond number is larger, i.e. for larger drops. By comparing the intersections of the asymptotic laws (the dashed lines in figure 5*a*) we find, indeed, this tendency proven.

While figure 5(*a*) accurately demonstrates the experimental findings, in figure 5(*b*) we compare the experimental data with theoretical predictions using the model of Ehrhard & Davis. These predictions are obtained for the appropriate Bond numbers $G = 2.4$, 7.6, 14.1 and transformed into physical units by using the scaling laws (2.5). The comparison demonstrates good agreement between prediction and experiment for all three drops within the complete observation interval of more than 5 hours. In particular the change in slope as time progresses (cf. figure 5*a*) is perfectly shown by the model predictions. Therefrom we conclude that the model of Ehrhard & Davis, and linked with it the main assumptions as summarized in §2, are appropriate to describe the isothermal spreading of such drops on horizontal surfaces.

The above findings on the isothermal spreading of silicone oil, including the effect of gravity, are not all new. Various authors have come to identical conclusions from experimental (cf. Cazabat & Cohen Stuart 1986) and from theoretical (cf. Ehrhard & Davis 1991) points of view. Our measurements within the isothermal set-up with a flow of ambient helium confirm, additionally, the negligible effect of the stagnant-point flow above the spreading drop. This can be included from our recovery of the typical time laws as found by other experimentalists using set-ups without an ambient flow. A quantitative comparison of the exponents in (4.1) and (4.2) will be made below in table 2.

In the next step we take our set of isothermal data and apply the scaling laws (2.5). Additionally, we include original data from Cazabat & Cohen Stuart (1986) and Chen (1988) and scale those accordingly. This procedure allows a scaled comparison of both a set of drops with vastly different viscosities and volumes, and our corresponding theoretical predictions. It should be mentioned that our knowledge of the fluid properties of the previous experiments is incomplete with respect to temperature dependencies. Therefore, scaling of these authors' data relies eventually on non-precise fluid properties.

Figure 6 shows, again in double-logarithmic coordinates, the non-dimensionalized drop radius $a(t)$ from the present experiments and from those of Cazabat & Cohen Stuart and Chen. The experiments are conducted in a Bond number range of

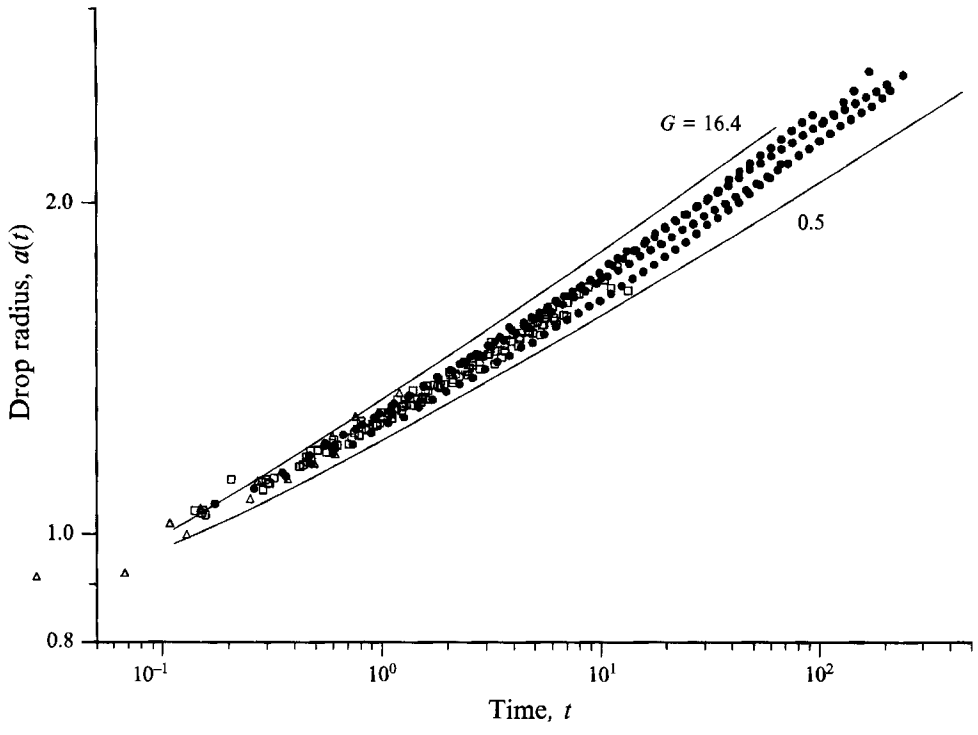

FIGURE 6. Isothermal spreading of silicone oil on glass, the perfectly wetting system: drop radius as function of time, in dimensionless form. Experimental data are included from Cazabat & Cohen Stuart (1986) (□) and Chen (1988) (△). Present experiments are given by symbols ●. Parameters for the theory (solid lines) are $M = 0$, $\Theta_A = 0$, $m = 2.8$.

Reference	Axisymmetric drops $a \propto t^n$		Dominant force	Viscosity (Pa s)
	$\bar{n}$	n		
Tanner (1979)	0.109	0.106–0.112	ST	1.008, 13.0
Cazabat & Cohen Stuart (1986)	0.105	0.094–0.125	ST	0.020, 1.0
	0.129	0.118–0.137	G	
Chen (1988)	0.106	0.080–0.123	ST	0.195
Present results	0.112	0.089–0.122	ST	0.125
	0.145	0.128–0.165	G	

TABLE 2. Isothermal spreading results for silicone oil on glass. ST and G denote surface-tension controlled and gravity-controlled, respectively

$0.5 \leqslant G \leqslant 16.4$ and therefore we get a family of experimental curves. By analysing those curves more closely we find that the lower curves belong to low Bond numbers and the upper curves to high Bond numbers. Thus, with very few exceptions, the curves are sorted with respect to Bond number.

These experimental findings are in accordance with the theoretical predictions. By varying the Bond number G within the model, we find a family of curves. The limiting curves for $G = 0.5$ and $G = 16.4$ are given as solid lines in figure 6. The model

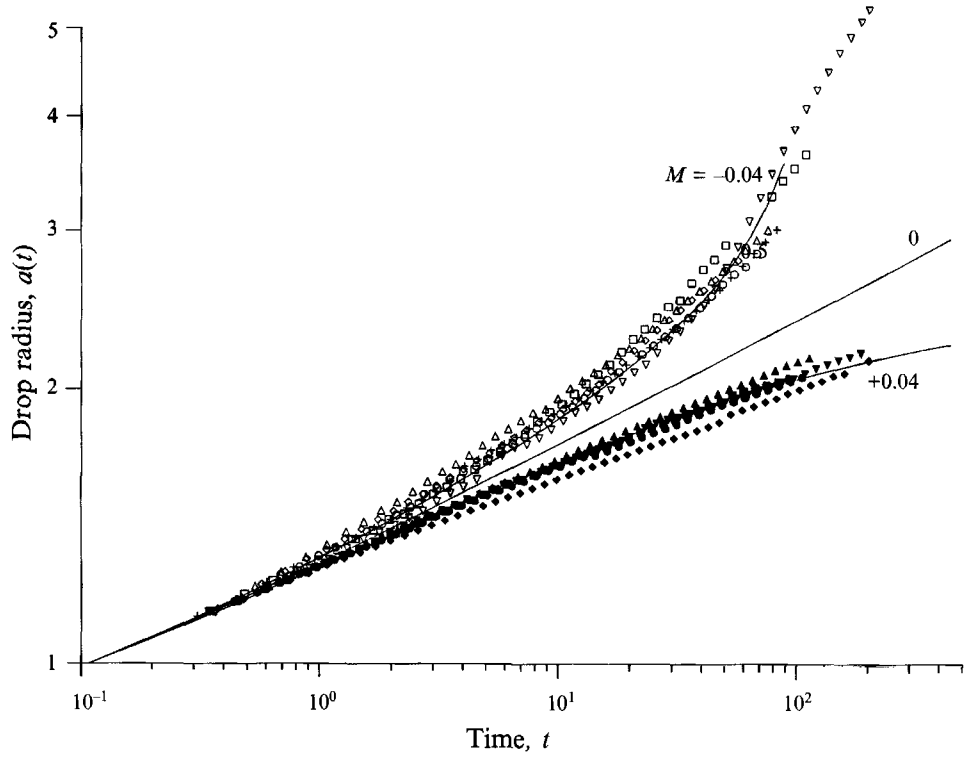

FIGURE 7. Non-isothermal spreading of silicone oil on glass, the perfectly wetting system: drop radius as function of time, in dimensionless form. Experimental data are given by closed symbols (heated plate) and open symbols (cooled plate). Parameters for the theory (solid lines) are $G = 10$, $\Theta_A = 0$, $m = 2.8$.

predictions and the experimental behaviour are in good agreement. The very few data points outside the theoretical range are from experiments by Cazabat & Cohen Stuart or Chen, for small times. As previously explained, those slight discrepancies might be attributed to non-precise knowledge of the relevant fluid properties. Moreover, during this early stage of spreading the initial drop shape may still have some influence. The initial drop shape, however, depends on the handling of the injection needle during positioning and therefore is variable.

In table 2 we show a comparison among the slopes obtained by various experimentalists. The corresponding viscosity range is $0.02 \leqslant \mu \leqslant 13.0$ Pa s. By regressing the experimental data to a model of type (4.1) and (4.2), the slopes can be inferred; these are valid within the capillary-dominated and the gravity-dominated regimes, respectively. For capillary-dominated spreading $0.105 \leqslant \bar{n} \leqslant 0.112$ is confirmed by all experimentalists, while for gravity-dominated spreading we get $0.129 \leqslant \bar{n} \leqslant 0.145$. As shown from figure 6, the present experiments cover, for the first time, a sufficient range in time to permit a reliable determination of the slope in the gravity-dominated regime.

4.2. *Non-isothermal conditions*

In figure 7 we present in an equivalent, non-dimensionalized form, our results for non-isothermal conditions. Two experimental families of curves are shown: open symbols relate to the cooled plate, while closed symbols relate to the heated plate. We recognize

a different behaviour of the drops depending on the thermal conditions. The cold plate obviously augments the spreading process while the hot plate retards it. Within each family of curves a range of Bond numbers is represented, owing to a variety of drop sizes: the lower curves correspond to small Bond numbers and the upper curves correspond to large Bond numbers. This means that within each family of drops, the curves again sort with Bond number. The actual range of Bond numbers is $1.5 \leqslant G \leqslant 14.2$.

For comparison we have included three theoretical curves calculated for an average Bond number of $\bar{G} = 10$ and three thermal conditions, namely the heated plate ($M = +0.04$), the cooled plate ($M = -0.04$) and the isothermal situation ($M = 0$). The latter represents essentially an average behaviour of all isothermally conditioned drops shown in figure 6. For clarity we do not include the ranges of Bond numbers, which would break up every solid curve into two range-limiting curves. The influence of the Bond number in this case is, however, identical to that described for the isothermal situation. If we compare the theoretical curves found for $M = \pm 0.04$, with the experimental data we find reasonable agreement. Deviations are only present for the case of the cooled plate at large times, where the model predicts a faster spreading than the experiments suggest. This discrepancy, observed for very thin liquid layers, might be attributed to three-dimensional effects which are described in §6.

As seen from figure 7, we get agreement between model and experiments for $M = \pm 0.04$. In contrast, our preliminary measurements (see §3.2) suggested values of $M = +0.085$ and $M = -0.06$, respectively, for the Marangoni number. Here a considerable discrepancy remains. In view of the method applied to determine the actual Marangoni number experimentally, these results should be taken only as order of magnitude determinations; such a method is strongly intrusive.

5. Results for paraffin oil/glass: limited spreading

In contrast to the experiments in §4, paraffin oil on glass exhibits partial wetting. Thus, given an initial contact angle $\theta_0 > \theta_A$ (cf. figure 4*b*) the drop is expected to spread ($a_t > 0$) until it approaches an actual contact angle $\theta \approx \theta_A$. As $t \to \infty$ we therefore expect a steady drop shape, whereas the final drop radius, a_∞, will be affected by the thermal conditions (i.e. by the Marangoni number M). The pertinent correlation, given by Ehrhard & Davis (1991), leads to a decrease (increase) of the final drop radius a_∞ if the plate is heated (cooled) with respect to the ambient gas.

5.1. *Non-isothermal conditions*

Our results for paraffin oil on glass, subject to non-isothermal conditions, are shown in figure 8, with closed symbols for the heated plate and open symbols for the cooled plate. We recognize an asymptotic approach for all curves to a steady final drop radius (note the logarithmic timescale). This result is characteristically different from the observations in the case of complete wetting (see §4). In particular for conditions of a heated (cooled) plate the drops spread more slowly (rapidly) and approach a smaller (larger) final radius. With different drop volumes, we realize a range of Bond numbers within these experiments, namely $G = 2.9$, 8.2 (heated plate) and $G = 2.7$, 14 (cooled plate). In contrast, the theoretical curves (solid lines) are calculated for an average Bond number of $\bar{G} = 10$ and Marangoni numbers $M = \pm 0.04$. As before, the lower experimental curves in both cases are associated with low Bond numbers. Thus the effect of gravity, which has been discussed in §4.1 for complete wetting, is completely analogous for the partially wetting experiments.

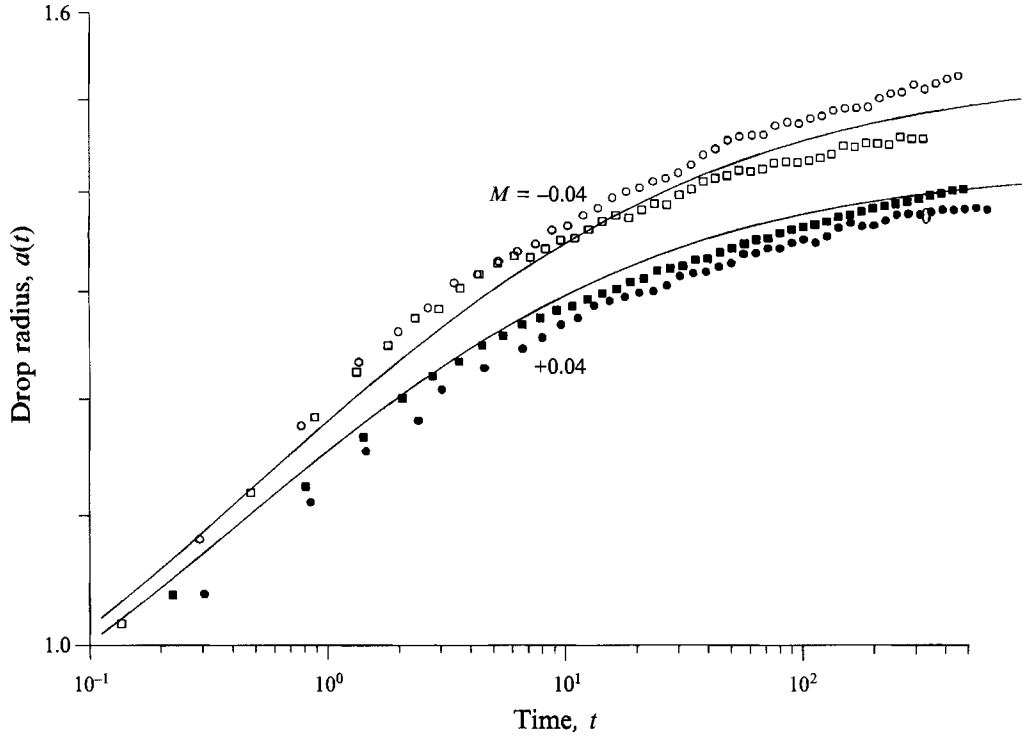

FIGURE 8. Non-isothermal spreading of paraffin oil on glass, the partially wetting system: drop radius as function of time, in dimensionless form. Experimental data are given by closed symbols (heated plate) and open symbols (cooled plate). Parameters for the theory (solid lines) are $G = 10$, $\Theta_A = 0.55$, $m = 2.8$.

Even though there are some imperfections with respect to the smoothness of the experimental curves, we detect a reasonable agreement between model predictions and experiments. In particular, the effect of Marangoni number M on both the time laws and the final drop radius is demonstrated. As discussed above, we assume a mobility exponent $m = 2.8$, as determined from the completely wetting experiments with silicone oil on glass, to be likewise valid for the paraffin oil experiments featuring partial wetting. The theoretical curves in figure 8 are computed using $m = 2.8$, but varying the mobility exponent within a range $2 \leqslant m \leqslant 3$ resulted in no major changes to the theoretical curves. Thus, the agreement would be valid for all these values of m, implying that a precise determination of the mobility exponent purely on the basis of our paraffin oil experiments (partial wetting) is hardly possible.

5.2. *Transient conditions*

In this section we focus our attention on the question of how the thermal conditions affect the approach towards a final steady state of the drop. For that reason we conduct an experiment with, initially, conditions of a heated plate ($M > 0$), which are expected to slow down the spreading and the drop will approach a 'small' final diameter. At $t \approx 55$ the temperature is changed, corresponding to a transition from conditions of a heated plate ($M > 0$) to those of a cooled plate ($M < 0$). For this transition we need a time span of $\Delta t \approx 32$. The start and end of the transient is marked in figure 9 by vertical dashed lines.

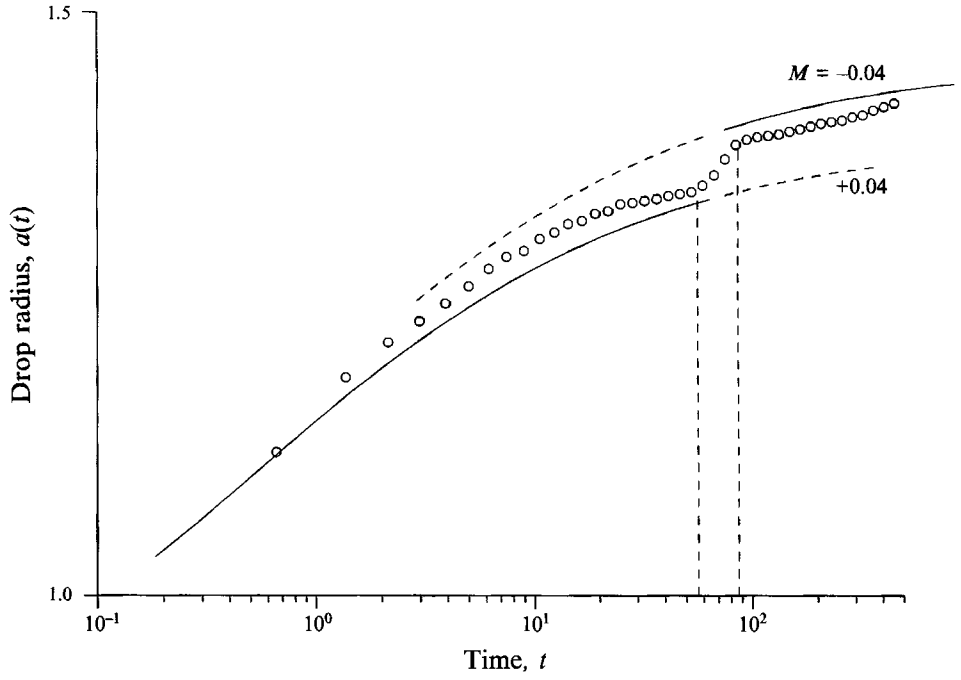

FIGURE 9. Transient experiment on paraffin oil on glass, the partially wetting system: drop radius as function of time, in dimensionless form. Experimental data are given by symbols ○; the start and end of the transient change of thermal conditions are marked by vertical dashed lines. Parameters for the theory (solid and dashed lines) are $G = 10$, $\Theta_A = 0.55$, $m = 2.8$.

The experimental data (open symbols) in figure 9 show the expected response of the drop to the change of thermal conditions. During the transient period a strong acceleration of the spreading occurs showing as a ramp-type time behaviour. Thus the approach towards a 'small' final drop radius (corresponding to the $M > 0$ case) is interrupted and an approach towards a 'large' final drop radius (corresponding to the $M < 0$ case) is developing. For comparison we have included solid lines corresponding to theoretical predictions for the cases $M = \pm 0.04$ and an average Bond number of $\bar{G} = 10$.

6. Three-dimensional effects

There are several situations that potentially lead to drops that no longer have circular shape. Firstly, if drops develop towards extended very thin liquid layers, one expects surface roughness to be of lengthscale similar to the layer thickness. This causes at first a more or less stochastic distortion of the ideally circular drop perimeter. Given such conditions, it is clear that a two-dimensional model will fail to describe the evolution of the drop. In fact, we occasionally have observed such 'rough' drop contours, and have discarded these data from further processing.

Secondly, Carles & Cazabat (1989) have found three-dimensional instabilities which occur during the 'accelerated' spreading of oil drops. They use an atmosphere saturated with a volatile compound in order to alter surface tension in a transient manner; this causes an 'acceleration' of the spreading. During our measurements those phenomena likewise occurred, sometimes for large times. In figure 10 we show two

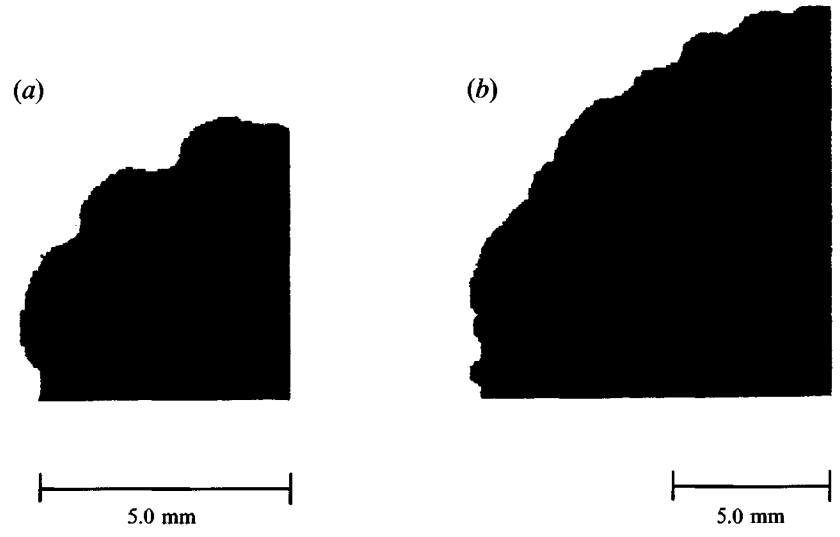

FIGURE 10. Examples of wavy instabilities at the drop circumference. One-quarter of the wetted area $\mathscr{A}(\ell)$ for each of two drops of different size are shown for silicone oil on glass, the completely wetting system, at a late stage.

examples of wavy instabilities at the drop circumference, as observed for two different drop sizes under isothermal conditions at large times. One-quarter of each drop of the completely wetting system silicone oil/glass is shown. A preliminary determination of the instability wavelength gives $\lambda_a = 2.0$ mm and $\lambda_b = 2.2$ mm, whereas a dependence on the drop radius is difficult to infer from our sparse data. Carles & Cazabat, though, have observed a weak increase of the wavelength with increasing drop radius, which we could confirm.

Our observations concerning these effects do not allow a clear judgement on under what conditions such instabilities occur; they have been observed more or less randomly for all thermal conditions, usually at large times. Since we have made comparisons to a two-dimensional model, we have ignored these data in all of our figures 5–10. A detailed experimental study on those effects is beyond the scope of the present investigation and beyond the capabilities of the techniques employed.

7. Discussion and conclusion

We have conducted experiments on the spreading of axisymmetric drops, subject to three different thermal conditions: (i) isothermal conditions, (ii) heated-plate conditions, (iii) cooled-plate conditions. Two classes of dynamic wetting behaviour have been examined, namely the completely wetting system of silicone oil/glass and the partially wetting system of paraffin oil/glass. The experimental data are used to validate the theoretical model proposed by Ehrhard & Davis (1991) in which the contact angle θ is related to contact-line speed U_{cl} by $U_{cl} = \kappa(\theta - \theta_A)^m$, the mobility capillary number is small, and lubrication theory applies.

7.1. *Unlimited spreading*

For the completely wetting system of silicone oil/glass under isothermal conditions, we confirm the results of Cazabat & Cohen Stuart (1986) and Chen (1988), who observed that after an initial transient, the spreading, which is capillary-controlled, develops

towards a gravity-controlled spreading with larger spreading rates. The time history of the position of the contact line (drop radius) $a(t)$ is in good agreement throughout the entire time interval with both previous experimental findings and theoretical predictions. The effect of gravity, as measured by the Bond number G, is affected by different initial drop volumes and material properties. It proves to be correctly reflected by the theory. The above observations with respect to isothermal conditions suggest a mobility exponent of $m \approx 2.8$. The data, moreover, demonstrates that the scaling laws (2.5) are adequate for comparing experiments with different drop volumes and viscosities.

The non-isothermal conditions lead to a retardation (augmentation) of the spreading when the plate is heated (cooled) with respect to the ambient gas. Thus, time histories for spreading under non-isothermal conditions are clearly distinguished from those under isothermal conditions. The effect of gravity is observed throughout each subgroup of curves, as large drops (large G) tend to enter the gravity-dominated regime at earlier times, and thus, spread faster. All the above experimental findings are in good agreement with the predictions of Ehrhard & Davis (1991), using $M = \pm 0.04$.

7.2. *Limited spreading*

A second set of experiments was performed using the partially wetting system of paraffin oil/glass. The experiments show, again, a retarded (augmented) spreading for the case of the heated (cooled) plate. The final radius approached is likewise affected by the thermal conditions; the drop spreads to a smaller (larger) radius if the plate is heated (cooled). The latter effect is clearly demonstrated by a transient experiment using one single drop. The predictions of Ehrhard & Davis (1991) relating to this situation give quantitative agreement if one takes $M = \pm 0.04$. Even though there is no direct measurement of the mobility exponent in this partially wetting system, there is evidence that $m = 2.8$ applies.

The present work, for the first time, experimentally confirms the influence of thermocapillary effects on the evolution of a spreading drop. We rely on measurements of the wetted area $\mathscr{A}(t)$, rather than measuring drop profiles, temperature fields or velocity fields. When the spreading is observed for very long times and/or very thin liquid layers one sees a substantial deviation from the axisymmetric drop. This is not surprising (cf. Carles & Cazabat 1989) and occurs through an either noisy or wavy disturbance at the drop circumference. This disturbance may lead to a three-dimensional instability, which, at least for larger amplitudes, limits the validity of the axisymmetric model.

There is the potential for a further instability to occur, namely a two-dimensional instability of the interface which maintains axisymmetry. Ehrhard & Davis (1991) have conjectured the existence of such a Marangoni instability in the heated-plate situation. However, we did not observe any indication of such an instability, though our measuring technique may not resolve small-amplitude waves at the interface.

The author gratefully acknowledges valuable discussion with S. H. Davis, Northwestern University (USA), during the course of this work. Moreover, he is indebted to G. Richter for running the experiments within the frame of his Diploma thesis at the University of Karlsruhe (FRG).

Appendix. Rescaling of the equations to allow for arbitrary volume

In the theory of Ehrhard & Davis (1991) their equations (3.14) and (3.18) involve the choosing of a specific drop volume (we employ their notation: p and a following equation numbers denote the two-dimensional and axisymmetric cases respectively), namely

$$V_0 = a_0^2 \theta_0, \tag{A 1p}$$

$$V_0 = a_0^3 \theta_0. \tag{A 1a}$$

It can be shown by using the following rescaling procedure that their set of equations is also valid for arbitrary drop volumes. We define a dimensionless drop volume as

$$V = V_0/a^2\theta_0, \tag{A 2p}$$

$$V = V_0/a^3\theta_0, \tag{A 2a}$$

and employ a modified set of dimensionless variables (with respect to their equation (3.1))

$$\left.\begin{gathered} \tilde{x} = \frac{x}{a_0}, \quad \tilde{r} = \frac{r}{a_0}, \quad \tilde{z} = \frac{z}{a_0 \theta_0 V}, \quad \tilde{t} = \frac{\kappa \theta_0^m V^m}{a_0} t, \\ \tilde{u} = \frac{u}{\kappa \theta_0^m V^m}, \quad \tilde{w} = \frac{w}{\kappa \theta_0^{(1+m)} V^{(1+m)}}, \quad \tilde{p} = \frac{a_0 \theta_0^{(2-m)} V^{(2-m)}}{\mu \kappa} p, \\ \tilde{T} = \frac{(T - T_\infty)}{(T_w - T_\infty)}, \quad \tilde{\Theta} = \frac{\theta}{\theta_0 V}, \end{gathered}\right\} \tag{A 3}$$

and find the complete set of equations unchanged except for their (3.13), which now reads

$$\tilde{h}_{0\tilde{x}}(1) = -1/V, \tag{A 4p}$$

$$\tilde{h}_{0\tilde{x}}(1) = -1/V, \tag{A 4a}$$

if the dimensionless parameter groups are redefined (with respect to their (3.20)) as

$$\left.\begin{gathered} C = \frac{\mu \kappa}{\sigma_w \theta_0^{(3-m)} V^{(3-m)}}, \quad G = \frac{\rho g a_0^2}{\sigma_w}, \quad B = \frac{\lambda_\infty a_0 \theta_0 V}{\lambda \delta}, \\ \Delta C = \frac{\mu \kappa}{\gamma (T_w - T_\infty) \theta_0^{(1-m)} V^{(1-m)}}, \quad \beta = \frac{\beta'}{a_0 \theta_0 V}. \end{gathered}\right\} \tag{A 5}$$

It can be easily proven that the case $V = 1$, which is equivalent to (A 1), transforms the present set (A 2)–(A 5) into the set of equations given by Ehrhard & Davis. From the modified scaling (A3) we can infer

$$\tilde{a} \propto V^{m/(2m+1)}, \tag{A 6p}$$

$$\tilde{a} \propto V^{m/(3m+1)}, \tag{A 6a}$$

for $\tilde{t} \to \infty$ (cf. Ehrhard & Davis, equation (6.6)). This dependency on the drop volume, at least for the axisymmetric case, is in accord with the findings of de Gennes (1985).

REFERENCES

CARLES, P. & CAZABAT, A. M. 1989 Spreading involving the Marangoni effect: some preliminary results. *Colloids Surfaces* **41**, 97.

CAZABAT, A. M. & COHEN STUART, M. A. 1986 Dynamics of wetting: effects of surface roughness. *J. Phys. Chem.* **90**, 5845.

CHEN, J.-D. 1988 Experiments on a spreading drop and its contact angle on a solid. *J. Colloid Interface Sci.* **122**, 60.

DUSSAN V., E. B. 1979 On the spreading of liquids on solid surfaces: static and dynamic contact lines. *A. Rev. Fluid Mech.* **11**, 371.

EHRHARD, P. & DAVIS, S. H. 1991 Non-isothermal spreading of liquid drops on horizontal plates. *J. Fluid Mech.* **229**, 365.

ELLIOTT, G. E. P. & RIDDIFORD, A. C. 1967 Dynamic contact angles. *J. Colloid Interface Sci.* **23**, 389.

FRIZ, G. 1965 Über den dynamischen Randwinkel im Fall der vollständigen Benetzung. *Z. Angew. Phys.* **19**, 378.

GENNES, P. G. DE 1985 Wetting: statics and dynamics. *Rev. Modern Phys.* **57**, 827.

GOODWIN, R. & HOMSY, G. M. 1991 Viscous flow down a slope in the vicinity of a contact line. *Phys. Fluids* A **3**, 515.

GREENSPAN, H. P. 1978 On the motion of a small viscous droplet that wets a surface. *J. Fluid Mech.* **84**, 125.

HOCKING, L. M. 1992 Rival contact-angle models and the spreading of drops. *J. Fluid Mech.* **239**, 671.

HOFFMAN, R. L. 1975 A study of the advancing interface. I. Interface shape in liquid–gas systems. *J. Colloid Interface Sci.* **50**, 228.

LEVINSON, P., CAZABAT, A. M., COHEN STUART, M. A., HESLOT, F. & NICOLET, S. 1988 The spreading of macroscopic droplets. *Rev. Phys. Appl.* **23**, 1009.

ROSE, W. & HEINS, R. W. 1962 Moving interfaces and contact angle rate-dependency. *J. Colloid Sci.* **17**, 39.

SCHWARTZ, A. M. & TAJEDA, S. B. 1972 Studies of dynamic contact angles on solids. *J. Colloid Interface Sci.* **38**, 359.

TANNER, L. H. 1979 The spreading of silicone oil drops on horizontal surfaces. *J. Phys.* D: *Appl. Phys.* **12**, 1473.